International Journal of Solids and Structures 46 (2009) 322–330

Contents lists available at ScienceDirect

International Journal of Solids and Structures

journal homepage: www.elsevier.com/locate/ijsolstr

Thickness effect of a thin film on the stress field due to the eigenstrain of an ellipsoidal inclusion

Xinghua Liang [a,b], Biao Wang [b,*], Yulan Liu [a]

[a] School of Engineering, Sun Yat-sen University, Guangzhou 510275, China
[b] Institute of Optoelectronic and Functional Composite Materials, School of Physics and Engineering, Sun Yat-sen University, Guangzhou 510275, China

ARTICLE INFO

Article history:
Received 1 March 2008
Received in revised form 18 August 2008
Available online 12 September 2008

Keywords:
Ellipsoidal inclusion
Eigenstrain
Stress field
Thin film
Thickness
Half-space

ABSTRACT

Solutions of the stress field due to the eigenstrain of an ellipsoidal inclusion in the film/substrate half-space are obtained via the Fourier transforms and Stroh eigenrelation equations. Based on the acquired solutions, the effect of a thin film's thickness on the stress field is investigated with two types of ellipsoidal inclusions considered. The results in this paper show that if the thickness of the thin film increases, its effect on the stress field will become weaker, and can even be neglected. In the end, a guide rule is introduced to simplify the calculation of similar problems in engineering.

1. Introduction

The film/substrate system has been widely used to model many physical and mechanical problems, which cover the areas of: piezoelectricity, thermomechanics, microelectronics, electronomagnetics, elastostatics, elastodynamics, and so on. In general, as the functional unit in the film/substrate system, the inclusion's properties can be significantly different, depending on the combined effects of film thickness, film surface, interface, eigenstrain and external stress field, etc. (Romanov et al., 2001; Li et al., 2002). With the rapid development in microminiaturization in the past few years, the effect of a film's thickness on the inclusions becomes more and more important, and is worth further study.

Ever since Kelvin found the first Green's function of a single point force in the infinite space in 1848, various elastic inclusion problems have been studied. Eshelby (1957, 1959) successfully solved the ellipsoidal inclusion problems in infinite space. The cuboidal inclusion problems have been solved by Chiu (1977). After Mindlin (1936) obtained the Green's function of a point force in semi-infinite space, the study of elastic problems was extended to half-spaces and bi-materials. At a later time, Green's function for joined half-spaces in perfect bond was established by Rongved (1955), and, for those in smooth contact, by Dundurs and Hetenyi (1965).

In recent years, multilayered elastic infinite and semi-infinite spaces have become the focus of a number of studies. Yuan et al. (2003) performed such a study of the three-dimensional Green's functions for composite laminates. Pan (1997, 2000), has done lots of work with bi-materials and multilayered half-spaces. Besides those of the point force, the solutions of several different force types in multilayered space were also studied, such as those of the ring force by Yue (1995) and the cone

* Corresponding author. Tel./fax: +86 20 84115692.
E-mail addresses: liangxh@mail2.sysu.edu.cn (X. Liang), wangbiao@mail.sysu.edu.cn (B. Wang), stslyl@mail.sysu.edu.cn (Y. Liu).

0020-7683/$ - see front matter © 2008 Elsevier Ltd. All rights reserved.
doi:10.1016/j.ijsolstr.2008.08.039

by Yue and Yin (1999). Krishnamurthy and Srolovitz (2004) came up with the general solution in thin films for two-dimensional stress distributions. Kolesnikova and Romanov (2004) developed a virtual circular dislocation–disclination loops technique for defects in solids, which can obtain the elastic fields and energies of a spherical dilatating inclusion or a prismatic dislocation loop in a plate and a half-space.

It is important to note that the research conducted on the topic of multilayered spaces, as well as the film/substrate half-space, mainly focused on single point force, or a ring force. Seldom has work been conducted to consider the stress field due to the eigenstrain of an ellipsoidal inclusion in the film/substrate half-space. In this paper, the authors successfully developed solutions for this problem, and investigated the effect of a thin film's thickness on the stress field. The formulas are based on the cylindrical system of vector functions and the solutions are expressed in terms of Fourier transforms. Two types of ellipsoidal inclusions were analyzed in this paper, and a guide rule was suggested to simplify the calculation of similar problems in the engineering field.

2. Problem description

For the time being, consider an isotropic film/substrate half-space with an ellipsoidal inclusion in the film. The origin of the Cartesian coordinate system is located on the film's surface. The distance from the top of the ellipsoidal inclusion to the surface is denoted d_1, while d_2 is the distance between the bottom of the ellipsoidal inclusion and the interface. Let t represent the thickness of the film. Three geometric parameters of the ellipsoidal inclusion are a_1, a_2, and a_3, as shown in Fig. 1.

In the absence of body forces, the differential equation of equilibrium in terms of displacements u_k is written as

$$C_{ijkl}u(x_1,x_2,z)_{k,lj}=0, \tag{1}$$

where i,j,k,l = 1,2,3, and C_{ijkl} is the elastic stiffness tensor.

For the purpose of this paper, the stress components are grouped into two types. They are called traction vector **t** and in-plane stress vector **s**, and respectively,

$$\mathbf{t}=(\sigma_{13},\sigma_{23},\sigma_{33})^{\mathrm{T}},\quad \mathbf{s}=(\sigma_{11},\sigma_{12},\sigma_{22})^{\mathrm{T}}. \tag{2}$$

Thus, the free boundary conditions at the film's surface can be written as

$$\mathbf{t}^{\mathrm{f}}=\mathbf{0}\quad \text{at } z=0; \tag{3}$$

and the bond conditions at the interface $z = t$ can be written as

$$\mathbf{u}^{\mathrm{f}}=\mathbf{u}^{\mathrm{s}},\quad \mathbf{t}^{\mathrm{f}}=\mathbf{t}^{\mathrm{s}}\quad \text{at } z=t, \tag{4}$$

since the displacements and tractions are required to be continuous here.

3. General solutions in the transformed domain

Applying two-dimensional Fourier transforms to Eq. (1)

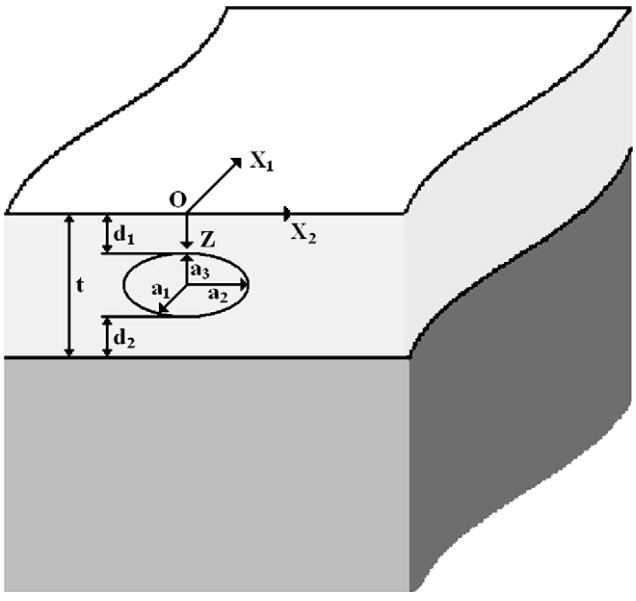

Fig. 1. An isotropic film/substrate half-space with an ellipsoidal inclusion.

$$\tilde{u}_i(y_1,y_2,z)=\int_{-\infty}^{\infty}\int_{-\infty}^{\infty}u(x_1,x_2,z)_i e^{i(x_1y_1+x_2y_2)}dx_1dx_2. \tag{5}$$

This can be revised as second-order ordinary differential equations with respect to z:

$$C_{i\alpha k\beta}y_\alpha y_\beta\tilde{u}_k+i\cdot(C_{i\alpha k3}+C_{i3k\alpha})y_\alpha\tilde{u}_{k,3}-C_{i3k3}\tilde{u}_{k,33}=0, \tag{6}$$

where $\alpha,\beta = 1,2$, and $i=\sqrt{-1}$.

In the following, we change the Cartesian coordinate system (y_1, y_2) to the polar coordinate system (r, θ). That is,

$$y_1=r\cdot n_1,\quad y_2=r\cdot n_2, \tag{7}$$

where $n_1 = \cos\theta$ and $n_2 = \sin\theta$. Then Eq. (6) can be revised as

$$r^2C_{i\alpha k\beta}n_\alpha n_\beta\tilde{u}_k+i\cdot r(C_{i\alpha k3}+C_{i3k\alpha})n_\alpha\tilde{u}_{k,3}-C_{i3k3}\tilde{u}_{k,33}=0. \tag{8}$$

A general solution of Eq. (8) is defined as

$$\tilde{\mathbf{u}}(y_1,y_2,z)=\mathbf{a}\cdot e^{-ipr z}, \tag{9}$$

and is substituted into Eq. (8). We then obtain the elastic Stroh eigenrelation equations in matrix form

$$[\mathbf{Q}+p(\mathbf{R}+\mathbf{R}^{\mathbf{T}})+p^2\mathbf{T}]\mathbf{a}=\mathbf{0}, \tag{10}$$

where

$$Q_{ij}=C_{i\alpha k\beta}n_\alpha n_\beta,\quad R_{ij}=C_{i\alpha k3}n_\alpha,\quad T_{ij}=C_{i3k3}, \tag{11}$$

and the superscript T denotes the transposition. Eq. (10) is the sixth polynomial in p, and the eigenvalues are either complex or purely imaginary. Once Eq. (10) is solved, the displacements can be easily obtained by Eq. (9).

The above results are the same as what Pan and Yuan completed in 2000 (Pan and Yuan, 2000), which focused on anisotropic materials. However, with regard to isotropic materials, we have:

$$C_{ijkl}=\lambda\delta_{ij}\delta_{kl}+G(\delta_{ik}\delta_{jl}+\delta_{il}\delta_{kj}), \tag{12}$$

where λ and G are Lame coefficients, and only two eigenvalues can be solved from Eq. (10): $p_1 = i$ and $p_2 = -i$ (triple roots). Thus, for each eigenvalue p, three non-correlation eigenvectors are needed to obtain the general solution of Eq. (8). Nevertheless, from Eqs. (9) and (10), only two pairs of non-correlation eigenvectors can be found, which are

$$\begin{cases}\mathbf{a}_1=[\sin\theta,-\cos\theta,0]^{\mathrm{T}}\\ \mathbf{a}_2=[0,-i,\sin\theta]^{\mathrm{T}}\end{cases},\quad p=i\qquad\text{and}\qquad\begin{cases}\mathbf{a}_1=[\sin\theta,-\cos\theta,0]^{\mathrm{T}}\\ \mathbf{a}_2=[0,i,\sin\theta]^{\mathrm{T}}\end{cases},\quad p=-i \tag{13}$$

To find the third pair of non-correlation eigenvectors, here we redefine the general solution (9) as

$$\tilde{\mathbf{u}}(y_1,y_2,z)=\mathbf{a}\cdot e^{-ipr z}+ir\cdot\mathbf{b}\cdot e^{-ipr z}. \tag{14}$$

Substituting it into Eq. (8), we then obtain the final pair of eigenvectors, which are

$$\begin{cases}\mathbf{a}_3=[0,0,3-4\mu]^{\mathrm{T}}\\ \mathbf{b}_3=[\cos\theta,\sin\theta,i]^{\mathrm{T}}\end{cases},\quad p=i\qquad\text{and}\qquad\begin{cases}\mathbf{a}_3=[0,0,3-4\mu]^{\mathrm{T}}\\ \mathbf{b}_3=[\cos\theta,\sin\theta,-i]^{\mathrm{T}}\end{cases},\quad p=-i \tag{15}$$

where μ is the Poisson ratio.

Now, the general solution of Eq. (8) is obtained, and can be further expressed as

$$\tilde{\mathbf{u}}=\mathbf{A}_1\langle e^{rz}\rangle\mathbf{v}+\mathbf{A}_2\langle e^{-rz}\rangle\mathbf{w}, \tag{16}$$

where $\langle e^{rz}\rangle = diag[e^{rz},e^{rz},e^{rz}]$, and $\mathbf{v}$ and $\mathbf{w}$ are unknown vectors to be determined by the boundary and bond conditions that will be mentioned in next section.

Matrix $\mathbf{A}_1$ and $\mathbf{A}_2$ are given, respectively, as

$$\mathbf{A}_1=\begin{bmatrix}\sin\theta & 0 & irz\cos\theta\\ -\cos\theta & -i & irz\sin\theta\\ 0 & \sin\theta & (3-4\mu)-rz\end{bmatrix},$$
$$\mathbf{A}_2=\begin{bmatrix}\sin\theta & 0 & i\cdot rz\cos\theta\\ -\cos\theta & i & i\cdot rz\sin\theta\\ 0 & \sin\theta & (3-4\mu)+rz\end{bmatrix}. \tag{17}$$

The formulae of $\mathbf{t}$ and $\mathbf{s}$ can be obtained by applying the stress–displacement relation in the transformed domain

$$\tilde{\sigma}_{ij} = -\mathrm{i}rn_\alpha C_{ijk\alpha}\tilde{u}_k + C_{ijk3}\tilde{u}_{k,3}, \tag{18}$$

as

$$\begin{aligned}\tilde{\mathbf{t}} &= -\mathrm{i}\cdot r(\mathbf{B}_1\langle \mathrm{e}^{rz}\rangle\mathbf{v} + \mathbf{B}_2\langle \mathrm{e}^{-rz}\rangle\mathbf{w})\\ \tilde{\mathbf{s}} &= -\mathrm{i}\cdot r(\mathbf{C}_1\langle \mathrm{e}^{rz}\rangle\mathbf{v} + \mathbf{C}_2\langle \mathrm{e}^{-rz}\rangle\mathbf{w})\end{aligned}, \tag{19}$$

where,

$$\begin{aligned}\mathbf{B_1} &= G\begin{bmatrix}\cos\theta\sin\theta & \mathrm{i}\cdot\sin\theta & 2(1-rz-2\mu)\cos\theta\\ 1+\sin^2\theta & -\mathrm{i}\cdot\cos\theta & 2(1-rz-2\mu)\sin\theta\\ \mathrm{i}\cdot 2\sin\theta & 0 & 2\mathrm{i}(2-rz-2\mu)\end{bmatrix},\\ \mathbf{B_2} &= G\begin{bmatrix}\cos\theta\sin\theta & -\mathrm{i}\cdot\sin\theta & 2(1+rz-2\mu)\cos\theta\\ 1+\sin^2\theta & \mathrm{i}\cdot\cos\theta & 2(1+rz-2\mu)\sin\theta\\ -\mathrm{i}\cdot 2\sin\theta & 0 & -2\mathrm{i}(2+rz-2\mu)\end{bmatrix},\\ \mathbf{C_1} &= G\begin{bmatrix}0 & \sin 2\theta & \mathrm{i}\cdot(rz+4\mu+rz\cos 2\theta)\\ -\mathrm{i}\cdot\cos\theta & -\cos 2\theta & \mathrm{i}\cdot rz\sin 2\theta\\ -\mathrm{i}\cdot 2\sin\theta & -\sin 2\theta & \mathrm{i}\cdot(rz+4\mu-rz\cos 2\theta)\end{bmatrix},\\ \mathbf{C_2} &= G\begin{bmatrix}0 & \sin 2\theta & \mathrm{i}\cdot(rz-4\mu+rz\cos 2\theta)\\ \mathrm{i}\cdot\cos\theta & -\cos 2\theta & \mathrm{i}\cdot rz\sin 2\theta\\ \mathrm{i}\cdot 2\sin\theta & -\sin 2\theta & \mathrm{i}\cdot(rz-4\mu-rz\cos 2\theta)\end{bmatrix}.\end{aligned} \tag{20}$$

In this section, the general displacement and stress solutions are successfully obtained in the Fourier transformed domain.

4. Solution of a single ellipsoidal inclusion in the film/substrate half-space

In this paper, the inclusion and the film are assumed to have the same elastic properties. The solution of the eigenstrain problem of a single ellipsoidal inclusion in infinite space is given by Eshelby (1957, 1959), denoting $\mathbf{u}^*$, $\mathbf{s}^*$ and $\mathbf{t}^*$ as displacement vector, in-plane stress vector and traction vector, respectively, with their Fourier transforms as $\tilde{\mathbf{u}}^*$, $\tilde{\mathbf{s}}^*$ and $\tilde{\mathbf{t}}^*$. If the elastic properties of the film and the inclusion are different, an artificial eigenstrain can be introduced to meet the different elastic properties of both phases (Eshelby, 1957; Mura, 1986).

The solutions of the film are assumed to have the following form:

$$\begin{aligned}\tilde{\mathbf{u}}^{\mathrm{f}}(r,\theta,z) &= \tilde{\mathbf{u}}^*(r,\theta,z) + \mathbf{A}_1^{\mathrm{f}}\langle \mathrm{e}^{rz}\rangle\mathbf{v}^{\mathrm{f}} + \mathbf{A}_2^{\mathrm{f}}\langle \mathrm{e}^{-rz}\rangle\mathbf{w}^{\mathrm{f}}\\ \tilde{\mathbf{t}}^{\mathrm{f}}(r,\theta,z) &= \tilde{\mathbf{t}}^*(r,\theta,z) - \mathrm{i}r(\mathbf{B}_1^{\mathrm{f}}\langle \mathrm{e}^{rz}\rangle\mathbf{v}^{\mathrm{f}} + \mathbf{B}_2^{\mathrm{f}}\langle \mathrm{e}^{-rz}\rangle\mathbf{w}^{\mathrm{f}}),\\ \tilde{\mathbf{s}}^{\mathrm{f}}(r,\theta,z) &= \tilde{\mathbf{s}}^*(r,\theta,z) - \mathrm{i}r(\mathbf{C}_1^{\mathrm{f}}\langle \mathrm{e}^{rz}\rangle\mathbf{v}^{\mathrm{f}} + \mathbf{C}_2^{\mathrm{f}}\langle \mathrm{e}^{-rz}\rangle\mathbf{w}^{\mathrm{f}})\end{aligned} \tag{21}$$

and the solutions of the substrate are assumed to be represented as

$$\begin{aligned}\tilde{\mathbf{u}}^{\mathrm{s}}(r,\theta,z) &= \mathbf{A}_1^{\mathrm{s}}\langle \mathrm{e}^{r(z-t)}\rangle\mathbf{v}^{\mathrm{s}} + \mathbf{A}_2^{\mathrm{s}}\langle \mathrm{e}^{-r(z-t)}\rangle\mathbf{w}^{\mathrm{s}}\\ \tilde{\mathbf{t}}^{\mathrm{s}}(r,\theta,z) &= -\mathrm{i}r(\mathbf{B}_1^{\mathrm{s}}\langle \mathrm{e}^{r(z-t)}\rangle\mathbf{v}^{\mathrm{s}} + \mathbf{B}_2^{\mathrm{s}}\langle \mathrm{e}^{-r(z-t)}\rangle\mathbf{w}^{\mathrm{s}}),\\ \tilde{\mathbf{s}}^{\mathrm{s}}(r,\theta,z) &= -\mathrm{i}r(\mathbf{C}_1^{\mathrm{s}}\langle \mathrm{e}^{r(z-t)}\rangle\mathbf{v}^{\mathrm{s}} + \mathbf{C}_2^{\mathrm{s}}\langle \mathrm{e}^{-r(z-t)}\rangle\mathbf{w}^{\mathrm{s}})\end{aligned} \tag{22}$$

The unknown vectors $\mathbf{v}^{\mathrm{f}}$, $\mathbf{m}^{\mathrm{f}}$, $\mathbf{v}^{\mathrm{s}}$ and $\mathbf{m}^{\mathrm{s}}$ can be determined by taking the boundary and bond conditions into consideration. Boundary condition (3) and bond condition (4) in the transformed domain can be expressed as

$$\tilde{\mathbf{t}}^{\mathrm{f}} = \mathbf{0} \quad \text{at } z = 0, \tag{23}$$

$$\tilde{\mathbf{u}}^{\mathrm{f}} = \tilde{\mathbf{u}}^{\mathrm{s}}, \qquad \tilde{\mathbf{t}}^{\mathrm{f}} = \tilde{\mathbf{t}}^{\mathrm{s}} \quad \text{at } z = t, \tag{24}$$

respectively. Considering that the substrate's thickness is infinite, Eq. (22) can be reduced to

$$\begin{aligned}\tilde{\mathbf{u}}^{\mathrm{s}}(r,\theta,z) &= \mathbf{A}_2^{\mathrm{s}}\langle \mathrm{e}^{-r(z-t)}\rangle\mathbf{w}^{\mathrm{s}}\\ \tilde{\mathbf{t}}^{\mathrm{s}}(r,\theta,z) &= -\mathrm{i}r\mathbf{B}_2^{\mathrm{s}}\langle \mathrm{e}^{-r(z-t)}\rangle\mathbf{w}^{\mathrm{s}}),\\ \tilde{\mathbf{s}}^{\mathrm{s}}(r,\theta,z) &= -\mathrm{i}r\mathbf{C}_2^{\mathrm{s}}\langle \mathrm{e}^{-r(z-t)}\rangle\mathbf{w}^{\mathrm{s}})\end{aligned} \tag{25}$$

since the displacement and stress components will be zero at the physically infinite.

Substituting Eqs. (23) and (24) into Eqs. (21) and (25), the unknown vectors $\mathbf{v}^{\mathrm{f}}$, $\mathbf{m}^{\mathrm{f}}$, $\mathbf{v}^{\mathrm{s}}$ and $\mathbf{m}^{\mathrm{s}}$ can be determined, and afterwards the solutions of a single ellipsoidal inclusion in the film/substrate half-space can be obtained in the transformed domain.

When solutions in the transformed domain are acquired, solutions in the physical domain can be easily obtained by carrying out the inverse Fourier transforms

$$u_i(x_1,x_2,z)=\frac{1}{(2\pi)^2}\int_{-\infty}^{\infty}\int_{-\infty}^{\infty}\tilde{u}_i(y_1,y_2,z)e^{-i(x_1y_1+x_2y_2)}dy_1\,dy_2 \quad . \tag{26}$$

5. Effect of a thin film's thickness on the stress field

To study the effect of a thin film's thickness on the stress field, we applied the previous formulation to the model described in Section 2. In this paper, the Poisson ratios of the film μ_1 and the substrate μ_2 are both 0.25, with shear moduli G_1 for the film and $G_2 = 5G_1$ for the substrate. The depth parameters d_1 and d_2 are set to the same variable d, which will change its value in the following analyses. The eigenstrain of the ellipsoidal inclusion is assumed to be uniformed dilatational, e.g. $\varepsilon_{ij} = \delta_{ij}\varepsilon^*$, in which ε^* is an arbitrary constant. Two types of ellipsoidal inclusions are discussed: in the first type, $a_1 = 3, a_2 = 2, a_3 = 5$ indicate a slim ellipsoidal inclusion; in the second type, $a_1 = 3, a_2 = 5, a_3 = 2$, they indicate a flat ellipsoidal inclusion.

In the process of computing, the discrete Fourier transform (DFT) and inverse discrete Fourier transform (IDFT) are adopted to substitute for the Fourier transforms and inverse Fourier transforms, in order to reduce the calculation time. The skill of performing the fast Fourier transform (FFT) is also used in this paper to accelerate the calculation. The results are presented in figures and tables, and are discussed below.

5.1. Comparison with FEM solutions

We first verify the solutions obtained in Section 4. The parameters of the ellipsoidal inclusion are set to $a_1 = 2, a_2 = 2, a_3 = 5$ so that the problem can be simplified to an axisymmetric model and can be solved easily with the finite element method (FEM). A comparison of the numerical results given by the current method and by FEM is shown in Fig. 2. This comparison indicates that the results given by the current method are reliable.

5.2. Results of type 1: a slim ellipsoidal inclusion ($a_1 = 3, a_2 = 2, a_3 = 5$)

As is shown clearly in Fig. 3, increasing the depth d decreases the stresses in the film/substrate system, especially for stresses near the surface and interface. As the depth d increases, the curves of stress components $\boldsymbol{\sigma}_{11}$, $\boldsymbol{\sigma}_{22}$ and $\boldsymbol{\sigma}_{33}$ in the film/substrate half-space are much more similar to what they will become in infinite space (d = infinite). As we can see in Fig. 3(a)–(c), curve $d = 10$ is so close to curve d = infinite that they appear to overlap. However, when the ellipsoidal inclusion is very close to the surface and interface, stress fields in the film are rather different than in infinite space. From Eshelby's work (1957,1959), we know that the stress components $\boldsymbol{\sigma}_{11}$, $\boldsymbol{\sigma}_{22}$ and $\boldsymbol{\sigma}_{33}$ are constant in the interior of the ellipsoidal inclusion in infinite space if the eigenstrain is uniformed dilatational; however, when the same inclusion is laid in the film, they do not keep constant anymore, which is obviously demonstrated from curves $d = 0.1$ and $d = 1$ in Fig. 3(a)–(c). We can also note that the stresses inside the ellipsoidal inclusion are more affected by the free-surface condition than by the restriction of the substrate with the higher shear modulus.

From Fig. 3, we also find that in the substrate, the stress component $\boldsymbol{\sigma}_{33}$ diminishes slower than $\boldsymbol{\sigma}_{11}$ and $\boldsymbol{\sigma}_{22}$ from the interface. With the exception of the stress component $\boldsymbol{\sigma}_{33}$, all curves of the stress components $\boldsymbol{\sigma}_{11}$ and $\boldsymbol{\sigma}_{22}$ have a rough jump when crossing the interface, which can be illustrated more clearly in Fig. 4; this shows the relationship between the depth of an ellipsoidal inclusion and the stress components on the center of the surface and interface.

5.3. Results of type 2: a flat ellipsoidal inclusion ($a_1 = 3, a_2 = 5, a_3 = 2$)

Though Fig. 5 shows similar patterns and trends as Fig. 3, the stress fields are greatly affected by the geometric change of the ellipsoidal inclusion. At the same depth d, the influence of the stress field on the flat ellipsoidal inclusion is stronger than

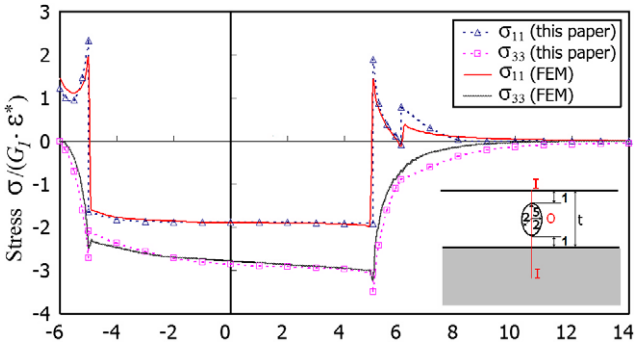

Fig. 2. Comparison between the current method and FEM.

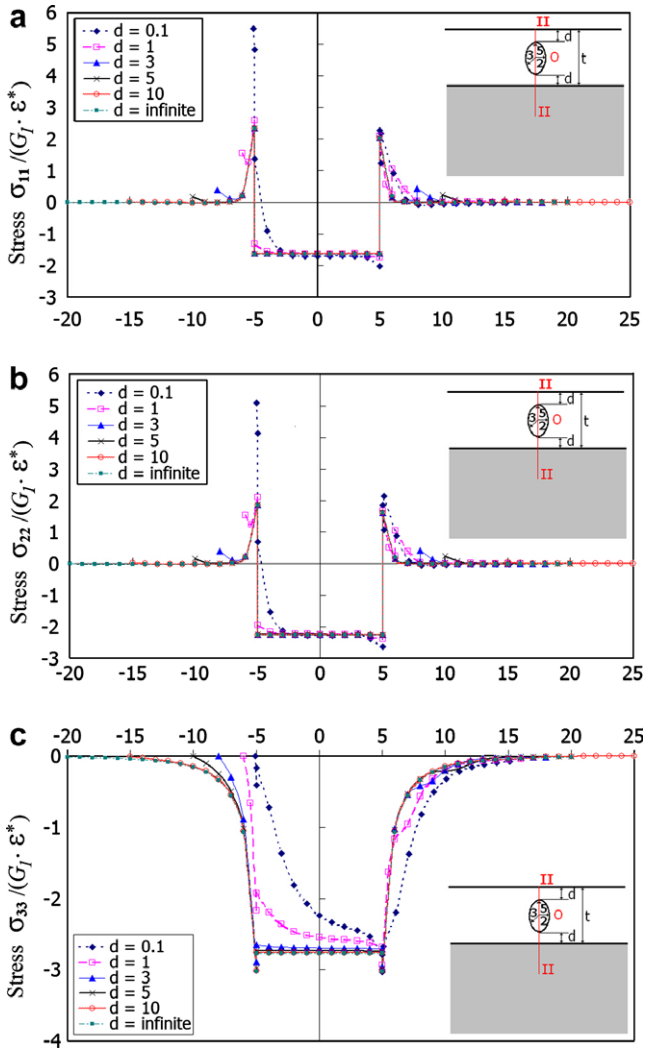

Fig. 3. Type 1's stress components along the z-axis (line II–II) at various depths d. (a) Normal stress $\boldsymbol{\sigma}_{11}$; (b) normal stress $\boldsymbol{\sigma}_{22}$; (c) normal stress $\boldsymbol{\sigma}_{33}$.

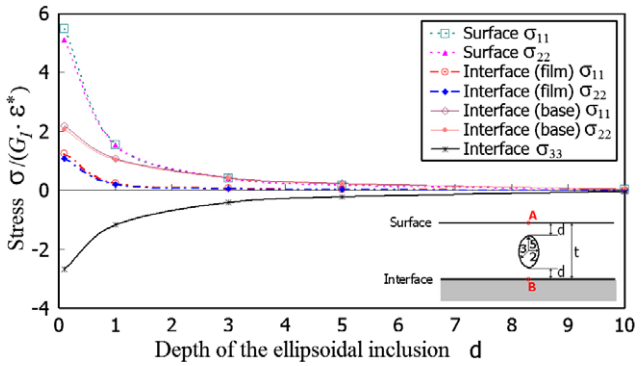

Fig. 4. Type 1's stress components at the center of the surface (point A) and the interface (point B) with the ellipsoidal inclusion at different depths d.

that on the slim ellipsoidal inclusion. However, for the same thickness t ($t = 2d + 2a_3$) of the film, the influence on the flat ellipsoidal inclusion is weaker than that on the slim one. Comparing Fig. 4 with Fig. 6, we can also easily note that, with the depth d increasing, the stress components in the former decrease faster than those in the latter.

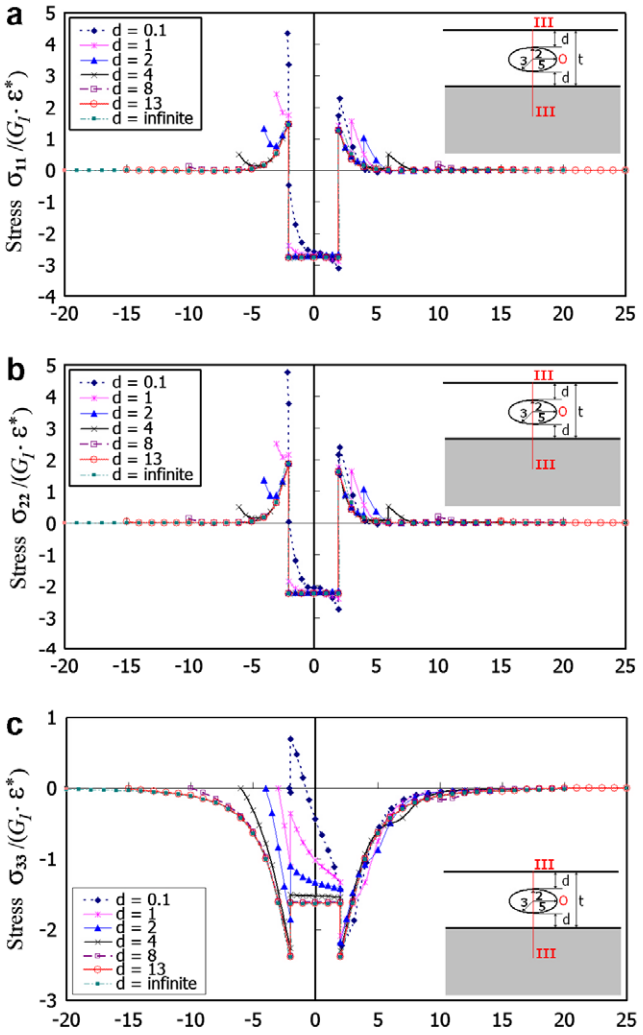

Fig. 5. Type 2's stress components along the *z*-axis (line III–III) at various depths *d*. (a) Normal stress $\boldsymbol{\sigma}_{11}$; (b) normal stress $\boldsymbol{\sigma}_{22}$; (c) normal stress $\boldsymbol{\sigma}_{33}$.

5.4. *Effect of a thin film's thickness*

As is shown in Figs. 3 and 5, increasing the depth *d* makes the curves of the stress components $\boldsymbol{\sigma}_{11}$, $\boldsymbol{\sigma}_{22}$ and $\boldsymbol{\sigma}_{33}$ in the film/substrate half-space more and more similar to what they will be in infinite space (*d* = infinite). For instance, the curve *d* = 10

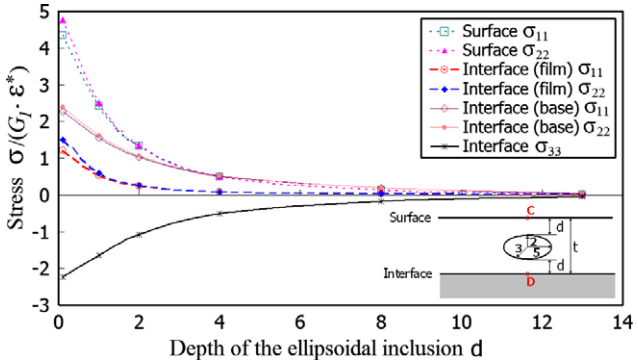

Fig. 6. Type 2's stress components at the center of the surface (point C) and the interface (point D) with the ellipsoidal inclusion at different depths *d*.

almost overlays the curve d = infinite in Fig. 3, and the curve d = 13 almost overlays the curve d = infinite in Fig. 5 in the region of the film. To give a quantitative description of these behaviors, Tables 1 and 2 list the values of the stress components in the films (t = 30) and infinite spaces for type 1 and type 2, respectively.

Except for those near the surface and interface, differences of the stress components in the film and in infinite space are no more than 32%, especially in the case of $\boldsymbol{\sigma}_{33}$ where the difference is less than 10%. Furthermore, the values of the stress components within the ellipsoidal inclusion in the film are very close to the values in infinite space, with differences of less than 1%. This shows the weak effect of a thin film's thickness on the stress field. In order to obtain such results, we find that depth d and parameters a_1, a_2, and a_3 need to satisfy following equation:

$$d + a_3 = 3\mathrm{Max}(a_1, a_2, a_3), \tag{27}$$

where d = 10 for type 1, and d = 13 for type 2.

Thus, in the general engineering calculation for the eigenstrain of an ellipsoidal inclusion in the film/substrate half-space: if the prospective stress components are not near the surface and interface, and such a formula is satisfied

$$\mathrm{Min}(d_1, d_2) + a_3 \geqslant k \cdot \mathrm{Max}(a_1, a_2, a_3), \tag{28}$$

where k = 3 here (or could be larger for more conservative results), the stresses in the infinite space can substitute as the stresses in the film for convenience-sake, without bringing in severe errors. The objective of Eq. (28) may be extended to general inclusions; in that case, however, its validity needs to be verified.

Table 1
Stress components in the film (t = 30) and in infinite space for type 1

z	$\boldsymbol{\sigma}_{11}$			$\boldsymbol{\sigma}_{22}$			$\boldsymbol{\sigma}_{33}$		
	Film	Infinite	Difference (%)	Film	Infinite	Difference (%)	Film	Infinite	Difference (%)
−15	0.0154	−0.0054	−387.29	0.0215	−0.0053	−509.85	−0.0103	−0.0430	−76.11
−12	−0.0053	−0.0095	−43.69	−0.0053	−0.0091	−42.03	−0.0718	−0.0871	−17.52
−9	−0.0114	−0.0153	−25.41	−0.0098	−0.0137	−28.19	−0.2134	−0.2248	−5.07
−6	0.1509	0.1476	2.21	0.1588	0.1555	2.11	−1.0575	−1.0683	−1.01
-5^-	2.3328	2.3297	0.13	1.8595	1.8564	0.17	−3.0126	−3.0233	−0.36
-5^+	−1.6340	−1.6380	−0.24	−2.2493	−2.2533	−0.18	−2.7646	−2.7753	−0.39
−3	−1.6344	−1.6380	−0.22	−2.2497	−2.2533	−0.16	−2.7648	−2.7753	−0.38
0	−1.6349	−1.6380	−0.19	−2.2502	−2.2533	−0.14	−2.7567	−2.7753	−0.67
3	−1.6351	−1.6380	−0.18	−2.2504	−2.2533	−0.13	−2.7652	−2.7753	−0.36
5^-	−1.6352	−1.6380	−0.17	−2.2505	−2.2533	−0.13	−2.7654	−2.7753	−0.36
5^+	2.0210	2.0191	0.09	1.6108	1.6089	0.12	−3.0134	−3.0233	−0.33
6	0.1391	0.1279	8.72	0.1367	0.1348	1.41	−1.0584	−1.0683	−0.93
9	−0.0120	−0.0133	−9.64	−0.0098	−0.0118	−17.06	−0.2153	−0.2248	−4.23
12	−0.0057	−0.0082	−30.65	−0.0053	−0.0079	−32.44	−0.0794	−0.0871	−8.82
15	−0.0036	−0.0046	−21.99	−0.0088	−0.0046	93.73	−0.0446	−0.0430	3.69

The origin is located at the center of the ellipsoidal inclusion as is shown in Fig. 3.

Table 2
Stress components in the film (t = 30) and in infinite space for type 2

z	$\boldsymbol{\sigma}_{11}$			$\boldsymbol{\sigma}_{22}$			$\boldsymbol{\sigma}_{33}$		
	Film	Infinite	Difference (%)	Film	Infinite	Difference (%)	Film	Infinite	Difference (%)
−15	0.0130	−0.0044	−394.91	0.0185	−0.0047	−495.73	−0.0090	−0.0377	−76.22
−12	−0.0047	−0.0083	−43.44	−0.0058	−0.0092	−36.95	−0.0786	−0.0900	−12.73
−8	−0.0072	−0.0105	−31.68	−0.0104	−0.0137	−24.07	−0.2006	−0.2104	−4.67
−5	0.0381	0.0352	8.15	0.0309	0.0281	10.06	−0.6333	−0.6429	−1.49
-2^-	1.4574	1.4549	0.17	1.8589	1.8564	0.13	−2.3821	−2.3915	−0.39
-2^+	−2.7721	−2.7753	−0.12	−2.2501	−2.2533	−0.14	−1.6286	−1.6380	−0.57
−1	−2.7722	−2.7753	−0.11	−2.2503	−2.2533	−0.14	−1.6287	−1.6380	−0.57
0	−2.7723	−2.7753	−0.11	−2.2504	−2.2533	−0.13	−1.6287	−1.6380	−0.57
1	−2.7724	−2.7753	−0.11	−2.2504	−2.2533	−0.13	−1.6288	−1.6380	−0.56
2^-	−2.7724	−2.7753	−0.10	−2.2505	−2.2533	−0.13	−1.6288	−1.6380	−0.56
2^+	1.2628	1.2609	0.15	1.6108	1.6089	0.12	−2.3823	−2.3915	−0.38
5	0.0324	0.0305	6.15	0.0261	0.0243	7.50	−0.6339	−0.6429	−1.40
8	−0.0072	−0.0091	−21.47	−0.0100	−0.0118	−15.87	−0.2017	−0.2104	−4.16
12	−0.0044	−0.0072	−38.50	−0.0055	−0.0080	−31.64	−0.0822	−0.0900	−8.65
15	−0.0029	−0.0038	−23.32	−0.0079	−0.0040	96.07	−0.0398	−0.0377	5.57

The origin is located at the center of the ellipsoidal inclusion as is shown in Fig. 5.

6. Conclusions

In this paper, we derived the formulation for calculating the stress field due to the eigenstrain of an ellipsoidal inclusion in the film/substrate half-space. The formulation is based on the cylindrical system of vector functions, and afterwards the solutions are expressed in terms of Fourier transforms. Two types of ellipsoidal inclusions, e.g. the slim ellipsoidal inclusion and the flat ellipsoidal inclusion, are discussed and compared in detail to study the effect of a thin film's thickness on the stress field. Numerical examples in this paper show that if a thin film's thickness increases, its effect on the stress field will become weaker, and could even be neglected. In the end, a guide rule is introduced to simplify the calculation of similar problems in the engineering field.

Acknowledgement

This work was supported by the National Natural Science Foundation of China (10572155, 10732100), and the Ministry of Education PRC Special Scientific Research Fund (20060558070).

References

Chiu, Y.P., 1977. On the stress field due to initial strains in a cuboid surrounded by an infinite elastic space. Journal of Applied Mechanics 44, 587–590.
Dundurs, J., Hetenyi, M., 1965. Transmission of force between two semi-infinite solids. Journal of Applied Mechanics 32, 671–674.
Eshelby, J.D., 1957. The determination of the elastic field of an ellipsoidal inclusion, and related problems. Proceedings of the Royal Society A241, 376–396.
Eshelby, J.D., 1959. The elastic field outside an ellipsoidal inclusion. Proceedings of the Royal Society A252, 561–569.
Kolesnikova, A.I., Romanov, A.E., 2004. Virtual circular dislocation–disclination loop technique in boundary value problems in the theory of defects. Journal of Applied Mechanics 71, 409–417.
Krishnamurthy, R., Srolovitz, D.J., 2004. A general solution for two-dimensional stress distributions in thin films. Journal of Applied Mechanics 71, 691–696.
Li, Y.L., Hu, S.Y., Liu, Z.K., Chen, L.Q., 2002. Effect of substrate constraint on the stability and evolution of ferroelectric domain structures in thin films. Acta Materialia 50, 395.
Mindlin, R.D., 1936. Force at a point in the interior of a semi-infinite solid. Physics 7, 195–202.
Mura, T., 1986. Micromechanics of Defects in Solids, 2nd revised ed. Martinus Nijhoff Publishers, Dordrecht.
Pan, E., 1997. Static Green's functions in multilayered half spaces. Applied Mathematical Modeling 21, 509–521.
Pan, E., Yuan, F.G., 2000. Three-dimensional Green's function in anisotropic bimaterials. International Journal of Structure and Solids 37, 5329–5351.
Romanov, A.E., Beltz, G.E., Fisher, W.T., Petroff, P.M., Speck, J.S., 2001. Elastic fields of quantum dots in subsurface layers. Journal of Applied Physics 89, 4523–4531.
Rongved, L., 1955. Force interior to one of two joined semi-infinite solids. In: Proceedings of the Second Midwestern Conference on Solid Mechanics, pp. 1–13.
Yuan, F.G., Yang, S., Yang, B., 2003. Three-dimensional Green's functions for composite laminates. International Journal of Solids and Structures 40, 331–342.
Yue, Z.Q., 1995. On generalized Kelvin solutions in a multilayered elastic medium. Journal of Elasticity 40, 1–43.
Yue, Z.Q., Yin, J., 1999. Layered elastic model for analysis of cone penetration testing. International Journal for Numerical and Analytical Methods in Geomechanics 23, 829–843.